AIAA JOURNAL
Vol. 38, No. 5, May 2000

Effects of Jet Temperature and Nozzle-Lip Thickness on Screech Tones

Hao Shen* and Christopher K. W. Tam†
Florida State University, Tallahassee, Florida 32306-4510

Imperfectly expanded supersonic jets, invariably, generate discrete frequency sound known as screech tones. In the low supersonic jet Mach-number range of 1.0–1.25, the screech phenomenon is axisymmetric. In this investigation the effects of jet temperature and nozzle-lip thickness on the axisymmetric jet screech modes are studied by numerical simulation. At the present time there is no known way to predict the intensities of screech tones, even empirically, except by numerical simulation. Numerical results of screech frequencies and directivities of heated jets will be reported. The computed screech frequencies are found to agree well with experimental measurements. Computed tone intensities indicate a gradual decrease in the screech amplitude with an increase in jet temperature. Screech tones are known to be sensitive to the presence of acoustic reflection surfaces. Sound reflected off such surfaces could sometimes affect the feedback loop that drives the screech tones. The nozzle lip is a good reflection surface. As a part of this work, the effect of nozzle-lip thickness on screech tone frequency and intensity is investigated. There are good agreements between the computed tone frequencies, intensities, and experiments at several nozzle-lip thickness to jet diameter ratios. Thick lip nozzles, as expected, are found to generate the loudest tones. But the change in sound-pressure level between a thin and a thick lip nozzle is found to be quite modest.

I. Introduction

SCREECH tones are discrete frequency sound emitted by imperfectly expanded supersonic jets.[1] Since the early work of Powell,[2] it has been known that these tones are generated by a feedback loop driven by the instability waves of the jet flow.[1,3] Over the years there have been numerous studies on the screech phenomenon. For references up to the early 1990s, the readers may consult Refs. 2 and 3. A more recent survey of the topic can be found in Ref. 4.

Most of the screech-tone experiments done in the past used jets with reservoir temperature T_r equal to the ambient temperature T_∞ (cold jets). There is, however, a general belief that, as the jet temperature increases, there is a corresponding decrease in the screech-tone intensity. In the literature there are only a few experimental and theoretical studies of screech tones from hot jets.[5–9] At low fully expanded supersonic jet Mach number ($M_j = 1.0$–1.25) the screech modes are axisymmetric. At higher Mach numbers the dominant screech modes are helical or flapping. An explanation of this mode switching phenomenon was offered recently by Tam et al.[6] They performed a total growth analysis of the axisymmetric, helical, and high-order azimuthal instability wave modes of jet flows at various Mach numbers and jet temperatures. They found that, at jet Mach numbers less than 1.25, the axisymmetric instability wave mode had the highest total growth. But, at higher Mach numbers, it was the helical mode that had the highest total growth. Because the instability wave is the energy source of the screech feedback loop, they suggested that the mode switching is associated with this change in instability wave characteristics.

Earlier, Tam et al.[10] had developed a formula for predicting the frequency of the flapping or helical mode screech. The formula has been found to compare well with the hot jet experimental measurements of Refs. 5–9. Reference 3 extended this formula to include the forward flight effect. Krothapalli et al.,[7] in their study of heated jets, compared the predicted tone frequencies of the extended formula with their measured data at flight Mach numbers up to 0.32. They found excellent agreement. For the axisymmetric jet screech modes Massey and Ahuja[8] proposed a semi-empirical frequency prediction formula by slightly modifying the formula of Ref. 10. The constants of the formula were adjusted by using the measured instability wave convection velocities.

Tam[1] has pointed out that no one has developed a formula for predicting the intensity of screech tones. Even a totally empirical formula is not available. At the present time the only way to predict screech-tone intensity is by numerical simulation.[11] In Ref. 11 numerical simulations were carried out only for cold jets. Appropriate modifications of the mathematical model are needed before the computer code can be applied to screech tones from hot jets.

Screech tones are known to be sensitive to changes in the external environment of the jet and the presence of sound reflection surfaces.[3] All of these factors can interfere with the basic screech feedback loop and hence affect the screech frequency and intensity. In a systematic investigation of screech suppression, Norum[12] was the first to observe the effect of nozzle-lip thickness on screech-tone intensity. There is a good reason to believe that nozzle-lip thickness should exert a considerable influence on screech-tone intensity. The nozzle lip is definitely an acoustic reflection surface. The reflection by the lip surface is important to the excitation of the instability wave that drives the screech. A more thorough investigation of nozzle-lip-thickness effect was carried out more recently by Ponton and Seiner.[13]

The objectives of the present investigation are twofold. First, we wish to investigate the effect of jet temperature on the screech frequency, intensity, and directivity. At the present time there is no reliable data on how jet temperature affects screech intensity and directivity. Our results would provide the first database in this respect. Second, it is our intention to offer an independent assessment of the effect of nozzle-lip thickness on screech-tone intensity. We will provide results that are in agreement with the measurements of Ponton and Seiner.[13]

The present investigation is based on numerical simulation. The approach is very similar to that of the author's earlier work.[11] To account for high-temperature effect on the turbulence in the mixing layer of the jet, the Sarkar correction[14,15] is included in the turbulence model. This will be discussed in Sec. II. Our study is confined to the Mach-number range of 1.0–1.25. Primarily, only the axisymmetric jet screech modes are studied.

Received 20 March 1999; revision received 27 July 1999; accepted for publication 27 September 1999.

*Postdoctoral Research Associate, Department of Mathematics. Member AIAA.

†Distinguished Research Professor, Department of Mathematics. Associate Fellow AIAA.

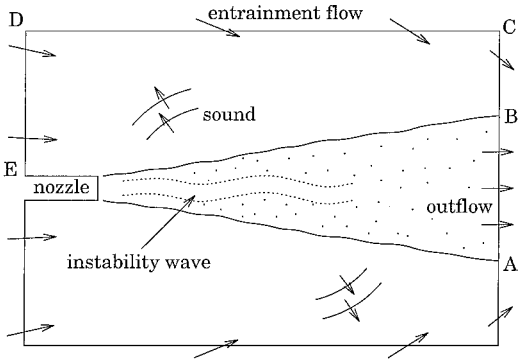

Fig. 1 Physical domain to be simulated.

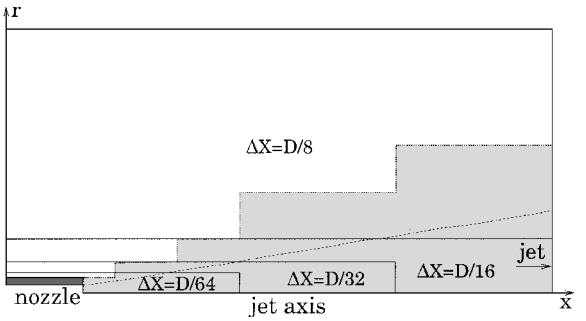

Fig. 2 Computation domain in the r–x plane showing the different subdomain and mesh sizes.

II. Mathematical Model and Computational Algorithm

The scope of this work is limited to the jet Mach-number range of 1.0–1.25 for which the screech modes are axisymmetric. Numerical simulations are carried out in the x–r plane, where (r, θ, x) are the cylindrical coordinates with the x axis coinciding with the jet axis. Figure 1 shows the physical domain to be simulated. The flow in the jet is turbulent. On following Ref. 11, no attempt will be made to resolve the many scales of turbulence. Instead, the effect of turbulence in the mixing layer of the jet is accounted for by including the k–ε turbulence model in the governing equations. However, for high-speed jets, especially at high temperature, it has been found experimentally that the efficiency of the mixing process is greatly reduced.[16,17] In Ref. 15 this effect is simulated by adding the Sarkar[14] correction, which was designed specifically for this purpose. We will use length scale $= D$ (nozzle exit diameter), velocity scale $= a_\infty$ (ambient sound speed), timescale $= D/a_\infty$, density scale $= \rho_\infty$ (ambient gas density), pressure scale $= \rho_\infty a_\infty^2$, and temperature scale $= T_\infty$ (ambient gas temperature); scales for k, ε, and ν_t are a_∞^2, a_∞^3/D, and $a_\infty D$, respectively. The dimensionless governing equations including the k–ε model and the Sarkar correction in Cartesian tensor notation are

$$\frac{\partial \bar\rho}{\partial t} + \frac{\partial \bar\rho \tilde u_j}{\partial x_j} = 0 \tag{1}$$

$$\frac{\partial \bar\rho \tilde u_i}{\partial t} + \frac{\partial \bar\rho \tilde u_i \tilde u_j}{\partial x_j} = -\frac{\partial \bar p}{\partial x_i} - \frac{\partial}{\partial x_j}(\bar\rho \tau_{ij}) \tag{2}$$

$$\frac{\partial \bar\rho E}{\partial t} + \frac{\partial}{\partial x_j}(\bar\rho E \tilde u_j) = -\frac{\partial}{\partial x_j}(\bar p \tilde u_j) - \frac{\partial}{\partial x_j}(\bar\rho \tilde u_i \tau_{ij}) + \frac{1}{P_r(\gamma-1)}\frac{\partial}{\partial x_j}\left(\bar\rho \nu_t \frac{\partial \tilde T}{\partial x_j}\right) + \frac{1}{\sigma_k}\frac{\partial}{\partial x_j}\left(\bar\rho \nu_t \frac{\partial k}{\partial x_j}\right) \tag{3}$$

$$\frac{\partial \bar\rho k}{\partial t} + \frac{\partial}{\partial x_j}(\bar\rho k \tilde u_j) = -\bar\rho \tau_{ij}\frac{\partial \tilde u_i}{\partial x_j} - \bar\rho\varepsilon + \frac{1}{\sigma_k}\frac{\partial}{\partial x_j}\left(\bar\rho \nu_t \frac{\partial k}{\partial x_j}\right) \tag{4}$$

$$\frac{\partial \bar\rho \varepsilon_s}{\partial t} + \frac{\partial}{\partial x_j}(\bar\rho \varepsilon_s \tilde u_j) = -C_{\varepsilon 1}\frac{\varepsilon_s}{(k+k_0)}\bar\rho \tau_{ij}^s \frac{\partial \tilde u_i}{\partial x_j} - C_{\varepsilon 2}\frac{\bar\rho \varepsilon_s^2}{(k+k_0)} + \frac{1}{\sigma_\varepsilon}\frac{\partial}{\partial x_j}\left(\bar\rho \nu_t^s \frac{\partial \varepsilon_s}{\partial x_j}\right) \tag{5}$$

$$\gamma \bar p = \bar\rho \tilde T \tag{6}$$

$$E = \frac{\tilde T}{\gamma(\gamma-1)} + \frac{1}{2}\tilde u_j^2 + k \tag{7}$$

$$\tau_{ij} = \frac{2}{3}k\delta_{ij} - \nu_t\left(\frac{\partial \tilde u_i}{\partial x_j} + \frac{\partial \tilde u_j}{\partial x_i} - \frac{2}{3}\frac{\partial \tilde u_k}{\partial x_k}\delta_{ij}\right) \tag{8}$$

$$\tau_{ij}^s = \frac{2}{3}k\delta_{ij} - \nu_t^s\left(\frac{\partial \tilde u_i}{\partial x_j} + \frac{\partial \tilde u_j}{\partial x_i} - \frac{2}{3}\frac{\partial \tilde u_k}{\partial x_k}\delta_{ij}\right) \tag{9}$$

$$\nu_t = C_\mu \frac{k^2}{(\varepsilon+\varepsilon_0)} + \frac{\nu}{a_\infty D}, \qquad \nu_t^s = C_\mu \frac{k^2}{(\varepsilon_s+\varepsilon_0)} + \frac{\nu}{a_\infty D} \tag{10}$$

$$\varepsilon = \varepsilon_s\left(1 + \alpha_1 M_T^2\right), \qquad M_T^2 = 2k/\tilde T \tag{11}$$

where $\bar{}$ denotes an ensemble average and $\tilde{}$ the Favre average. γ is the ratio of specific heats and ν is the molecular kinematic viscosity. The constants $k_0 = 10^{-6}$ and $\varepsilon_0 = 10^{-4}$ are small positive numbers added to prevent division by zero. The model constants are taken to be[15]

$$C_\mu = 0.0874, \quad C_{\varepsilon 1} = 1.40, \quad C_{\varepsilon 2} = 2.02$$
$$P_r = 0.422, \quad \sigma_k = 0.324, \quad \sigma_\varepsilon = 0.377$$
$$\alpha_1 = 0.518$$

The preceding equations are discretized according to the seven-point stencil dispersion-relation-preserving scheme.[18,19] The grid design is identical to Ref. 11. Figure 2 shows the computational domain. Four mesh sizes are used. The finest mesh with $\Delta x = \Delta r = D/64$ is in the block immediately downstream of the nozzle exit and enclosing the nozzle. Going out from the jet to the ambient region, the mesh size of the adjacent block increases by a factor of two. The domain extends 5 diameters back from the nozzle exit and 35 diameters long in the x direction. It is 17 diameters in the r direction. For the regions shaded gray in Fig. 2, the preceding governing equations are solved. This region contains the jet flow. Outside this region, the white region in Fig. 2, the disturbances are mainly acoustic waves. Viscous effects are unimportant. In this region the full Euler equations are solved. The treatment of the buffer zone between different blocks shown in Fig. 2, as well as the distribution of artificial selective damping, are the same as in Ref. 11. The boundary conditions around the computational domain and the wall boundary conditions also follow those of Ref. 11. For a more detailed description of these boundary conditions, the readers are referred to Ref. 20.

For all hot-jet simulations the nozzle lip is fixed at a thickness equal to half the jet diameter. For the lip-thickness-effect investigation three thicknesses are used. They are 0.5, 0.25, and $0.125D$. In each simulation the initial conditions are set equal to zero. At time equal to zero, the jet flow is allowed to enter the computational domain from the nozzle exit. The process is identical to turning the jet on in a physical experiment. The numerical solution is marched in time until the jet flow is developed, and the transient disturbances have entirely left the computation domain. The screech feedback loop automatically locks itself in the computation. The screech-tone frequency, intensity, and directivity are measured only when a time periodic state is fully established.

III. Effect of Jet Temperature

Screech tones are generated by the interaction between the large-scale instability waves of the jet flow and the shock cell structure in the jet plume.[1,3] To obtain an idea of the effect of jet temperature on screech tones, one may start by first examining its effect on the instability waves and on the shock cells. At a fixed jet Mach

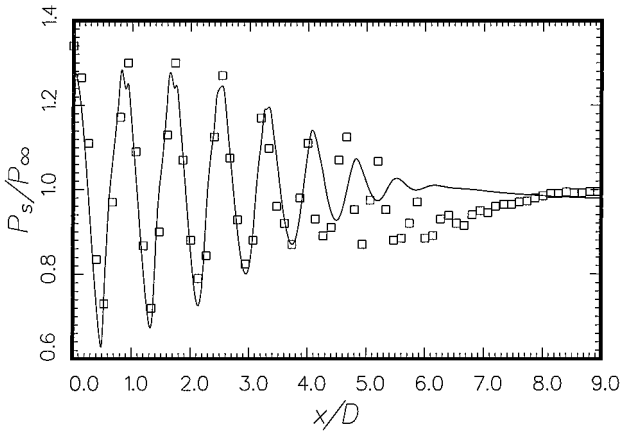

Fig. 3 Comparison between computed and measured[15] jet centerline pressure distributions: $M_j = 1.2$ and $T_r/T_\infty = 1.0$.

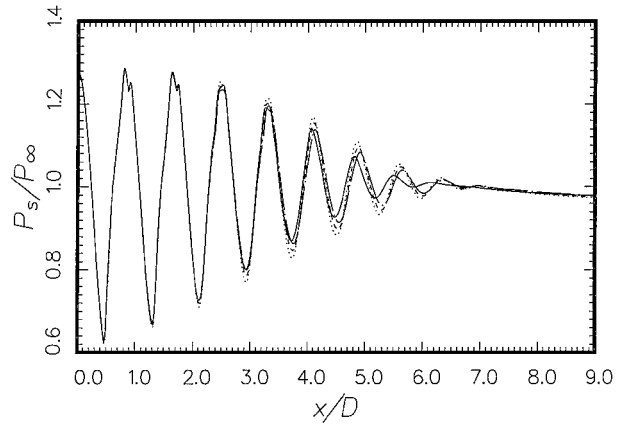

Fig. 4 Computed jet centerline pressure distributions at four temperature ratios: $M_j = 1.2$; ——, $T_r/T_\infty = 1.0$; – –, $T_r/T_\infty = 1.67$; – – –, $T_r/T_\infty = 2.37$; and · · ·, $T_r/T_\infty = 2.78$.

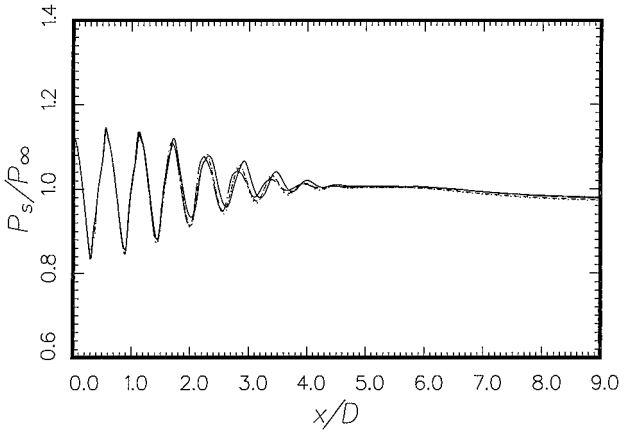

Fig. 5 Computed jet centerline pressure distributions at four temperature ratios: $M_j = 1.1$; ——, $T_r/T_\infty = 1.0$; – –, $T_r/T_\infty = 1.67$; – – –, $T_r/T_\infty = 2.37$; and · · ·, $T_r/T_\infty = 2.78$.

number the velocity of a hot jet is higher. As a result, the instability waves would propagate downstream at a higher speed. On the other hand the shock cells are Mach-number dependent, not temperature dependent. That is, jet temperature has little influence on shock cell spacings and amplitude. Figure 3 is a comparison of the computed and measured[21] jet centerline static pressure distribution for a jet from a convergent nozzle at $M_j = 1.2$ and $T_r/T_\infty = 1.0$. As can be seen for the first five shock cells, there is excellent agreement. Figure 4 gives the centerline pressure distributions of the same jet at four temperature ratios; $T_r/T_\infty = 1.0$, 1.67, 2.37, and 2.78. For the first five shock cells there is very little difference both in spacing and in amplitude. Figure 5 is a similar comparison at jet Mach

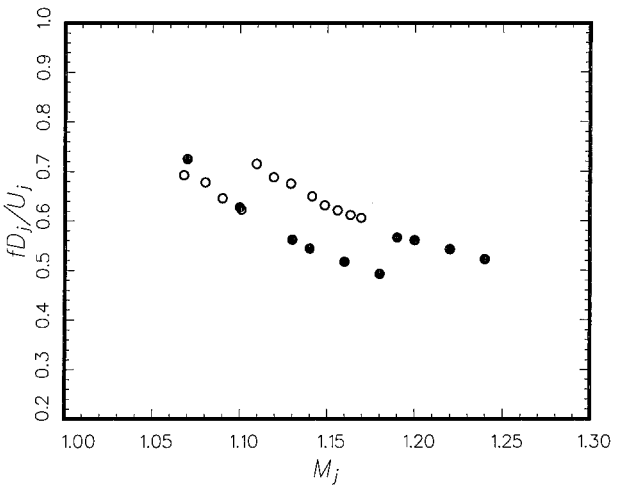

Fig. 6 Comparison between measured screech-tone frequencies from experiment and simulation. $T_r/T_\infty = 1.0$. Lower set of data is the A_1 mode; the higher frequency data are the A_2 mode: ○, experiment,[13] and ●, simulation.

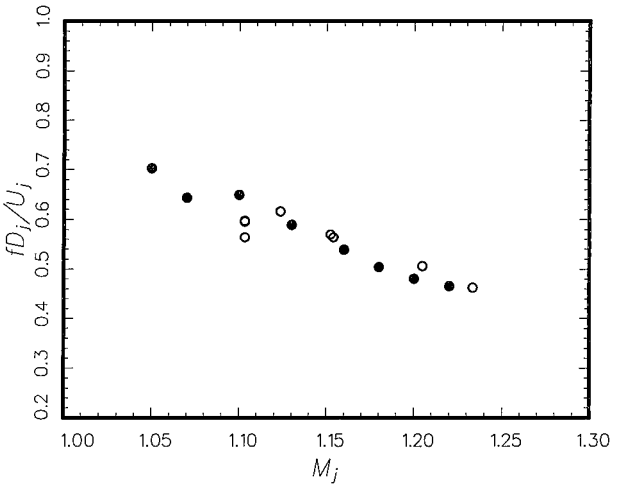

Fig. 7 Comparison between measured screech-tone frequencies from experiment and simulation. $T_r/T_\infty = 1.67$: ○, experiment,[8,9] and ●, simulation.

number 1.1. Again, the shock cell spacings and amplitudes are nearly independent of temperature.

Because the shock cell spacing is unaffected by an increase in jet temperature and the instability waves propagate faster downstream, the screech frequency must become higher. This is found both in the experiments of Massey and Ahuja[8] and Massey[9] and in the present simulations. However, in terms of Strouhal number $f D_j/u_j$, where f is the tone frequency and D_j and u_j are the fully expanded jet diameter and velocity, there is no large variation with jet temperature. Figures 6–9 show comparisons of the measured screech-tone frequency as a function of jet Mach number from the experiments of Ponton and Seiner,[13] Massey and Ahuja,[8] and Massey[9] and the present simulations. The temperature ratios are 1.0, 1.67, 2.37, and 2.78. There are good agreements between physical and computational experiments for all four temperature ratios. In the Massey and Ahuja experiments the absolute level of the screech-tone intensity was not reported.[8,9] However, in the nozzle-lip-thickness-effect experiments of Ponton and Seiner,[13] the screech-tone intensities were measured at $T_r/T_\infty = 1.0$. It will be shown later that there is good agreement between their measurements and our numerical simulations.

Figure 10 shows the computed directivity of screech tone intensity at $M_j = 1.13$ measured at a radial distance of $R = 65D$. The jet flow is from left to right. There are two basic lobes in the directivity pattern. The lobe pointing upstream is formed by the acoustic waves associated with the screech feedback loop. The computed

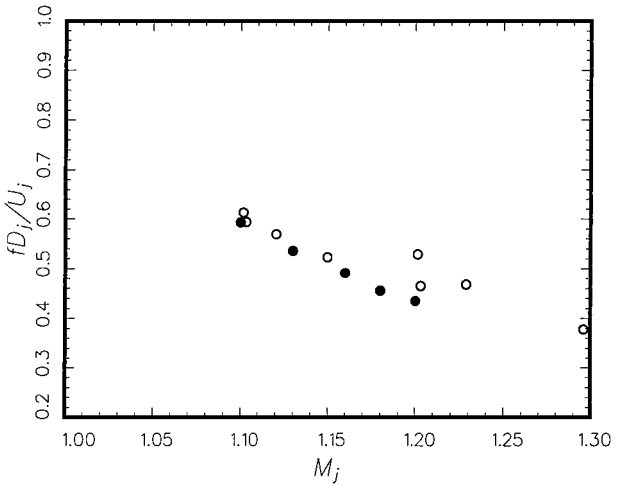

Fig. 8 Comparison between measured screech-tone frequencies from experiment and simulation. $T_r/T_\infty = 2.37$: ○, experiment,[8,9] and ●, simulation.

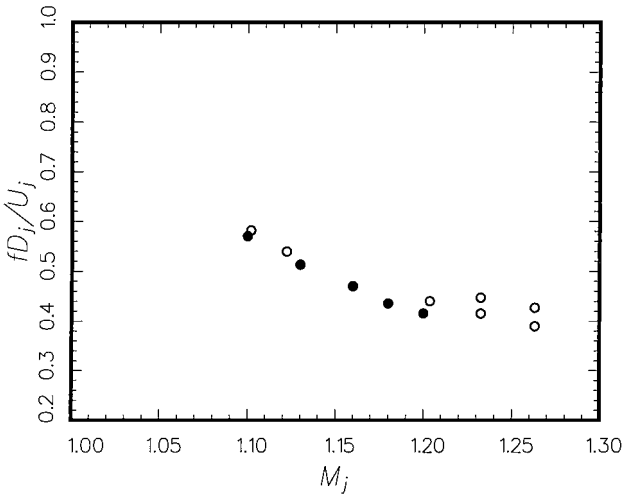

Fig. 9 Comparison between measured screech-tone frequencies from experiment and simulation. $T_r/T_\infty = 2.78$: ○, experiment,[8,9] and ●, simulation.

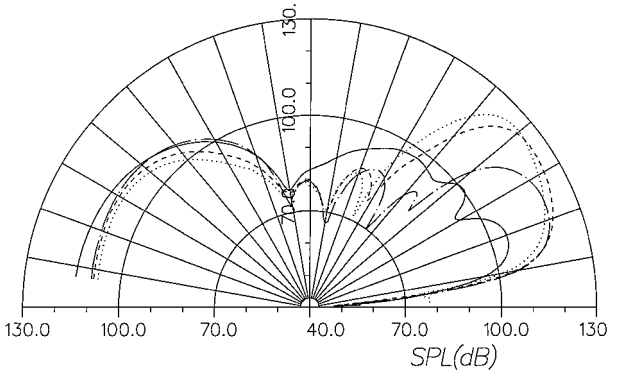

Fig. 10 Computed directivity distributions of the screech-tone intensity at $M_j = 1.13$ and $r = 65D$: ——, $T_r/T_\infty = 1.00$; – –, $T_r/T_\infty = 1.67$; – – –, $T_r/T_\infty = 2.37$; and · · ·, $T_r/T_\infty = 2.78$.

results indicate that there is a slight decrease in screech intensity with an increase in jet temperature at a fixed Mach number. This is consistent with the prevailing expectation. The other lobe points in the downstream direction. In Ref. 11 this lobe is not part of the screech feedback loop. It is sound or Mach waves generated directly by the instability waves. At a higher jet temperature the jet velocity as well as the speed of propagation of the instability waves increase. These cause stronger Mach wave radiation, a well-known fact in turbulent mixing noise studies. In addition, the Mach wave angle becomes larger so that the angle between the peak radiation direction and the direction of jet flow also increases. The computed directivities of Fig. 10 exhibit exactly these behaviors.

IV. Effect of Nozzle-Lip Thickness

In the experiments of Norum,[12] it was reported that a large increase in the mode C screech intensity, of the order of 10 dB, was observed by the use of a thick instead of a thin lip nozzle. On the other hand, in the experiments of Ponton and Seiner,[13] for this same mode the screech intensity is quite erratic when a thin lip nozzle was used. The purpose of the present investigation is to provide an independent assessment of the magnitude of the effect of nozzle-lip thickness. Since both Norum and Ponton and Seiner used cold jets in their experiments, the temperature ratio T_r/T_∞ of the jets in the present computational study will be set equal to unity. Three nozzle-lip thicknesses are used. They are $t/D = 0.5, 0.25$, and 0.125, where t is the thickness. The $t/D = 0.5$ case is a good representation of a thick lip nozzle. $t/D = 0.125$ case is a model for a thin lip nozzle.

In Norum's work variations of the screech-tone frequency and intensity with nozzle-lip thickness at low supersonic jet Mach number were not measured. Only the changes in decibel level relative to the thick lip nozzle were provided. For this reason the present effort will only compare the computed tone frequencies and intensities with the measurements of Ponton and Seiner.[13] Figure 11 shows a comparison between the acoustic wavelengths of the simulated screech tones and the data of Ponton and Seiner[13] for the thick lip nozzle. As can be seen, there is good agreement for both the A_1 and A_2 modes. The staging Mach number is, however, slightly higher in the computation results. Figures 12 and 13 show similar comparisons for the intermediate ($t/D = 0.25$) and the thin ($t/D = 0.125$) lip nozzles. Again, there are good agreements in the screech-tone acoustic wavelengths for both the A_1 and A_2 modes. In these cases even the staging Mach numbers are reproduced in the simulations.

Figure 14 is a comparison of the screech-tone intensity for the thick lip nozzle. The measurements are recorded by surface-mounted transducers at $r/D = 0.889$ and 0.642 on the nozzle lip surface. There are excellent agreements on the peak sound-pressure level (SPL) of the screech tones between the experiments and the simulations at both transducer locations. Figure 15 shows similar comparisons for the $t/D = 0.25$ nozzle. The SPLs are measured at $r/D = 2.0$ and 0.642, respectively. The SPL for the A_1 mode is in excellent agreement. The simulated SPL is somewhat lower than those of the experiment for the A_2 mode. Overall, the agreement is good. Figure 16 provides the results for the thin lip nozzle measured at $r/D = 2.0$. Except for a small range of Mach numbers around $M_j = 1.175$, the SPL of the simulation agrees well with the experimental measurements. Based on both the screech-tone frequency and intensity comparisons, it appears that the numerical simulation

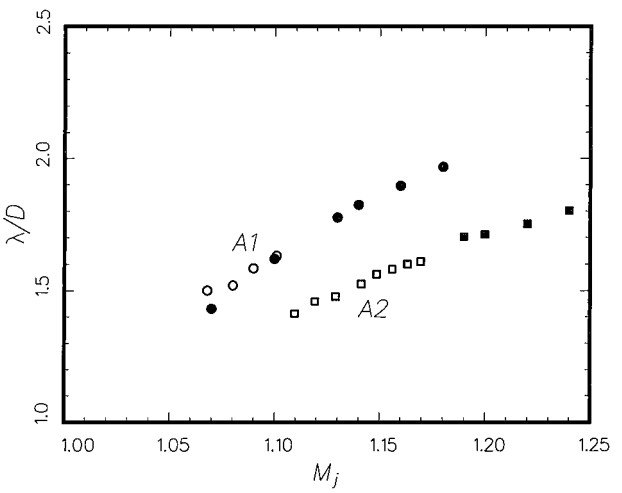

Fig. 11 Comparison between the acoustic wavelengths of simulated screech tones and the measurements of Ponton and Seiner[13]: ○ and □, experiment ($t/D = 0.625$); ● and ■, simulation ($t/D = 0.5$).

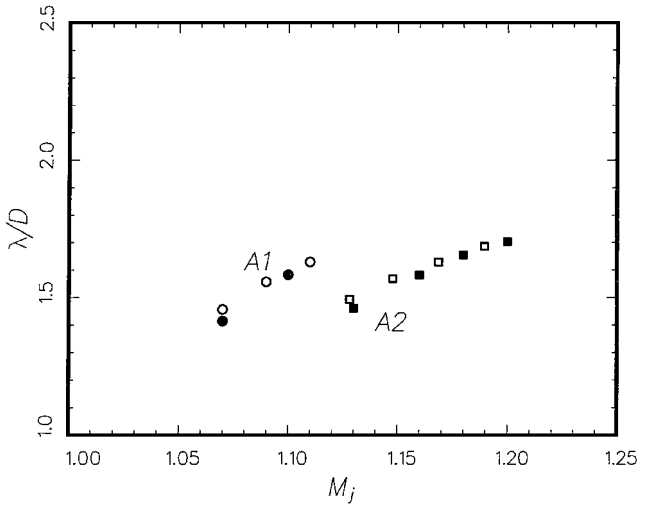

Fig. 12 Comparison between the acoustic wavelengths of simulated screech tones and the measurements of Ponton and Seiner[13]: ○ and □, experiment ($t/D = 0.2$); ● and ■, simulation ($t/D = 0.25$).

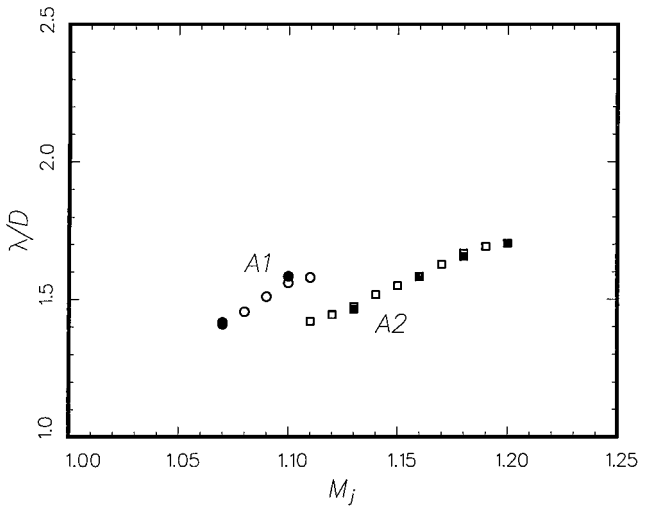

Fig. 13 Comparison between the acoustic wavelengths of simulated screech tones and the measurements of Ponton and Seiner[13]: ○ and □, experiment ($t/D = 0.1$); ● and ■, simulation ($t/D = 0.125$).

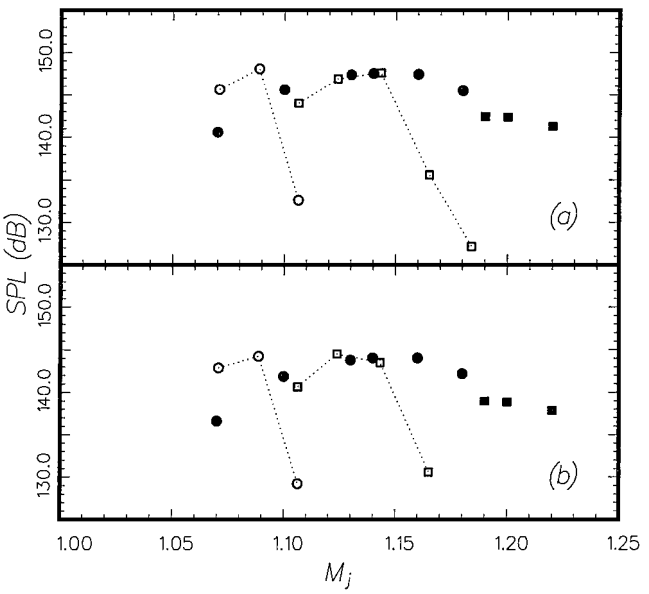

Fig. 14 Intensity of axisymmetric screech tones at nozzle exit plane: a) $r/D = 0.642$ and b) $r/D = 0.889$. Experiment[13] ($t/D = 0.625$): ○, A_1 mode and □, A_2 mode. Numerical simulation ($t/D = 0.5$): ●, A_1 mode, and ■, A_2 mode.

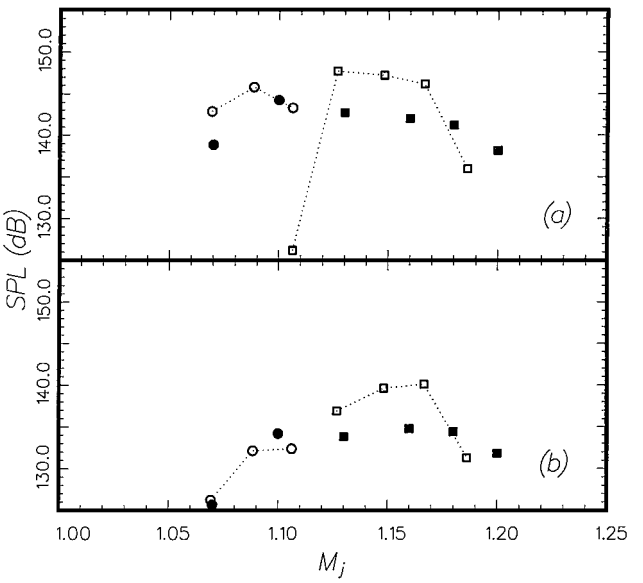

Fig. 15 Intensity of axisymmetric screech tones at nozzle exit plane: a) $r/D = 0.642$ and b) $r/D = 2.0$. Experiment[13] ($t/D = 0.2$): ○, A_1 mode and □, A_2 mode. Numerical simulation ($t/D = 0.25$): ●, A_1 mode, and ■, A_2 mode.

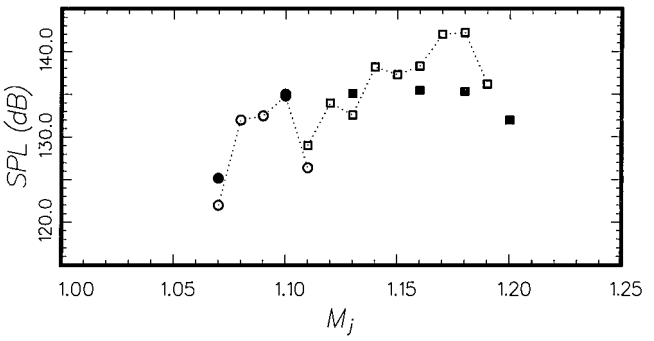

Fig. 16 Intensity of axisymmetric screech tones at nozzle exit plane: $r/D = 2.0$. Experiment[13] ($t/D = 0.1$): ○, A_1 mode, and □, A_2 mode. Numerical simulation ($t/D = 0.125$): ●, A_1 mode, and ■, A_2 mode.

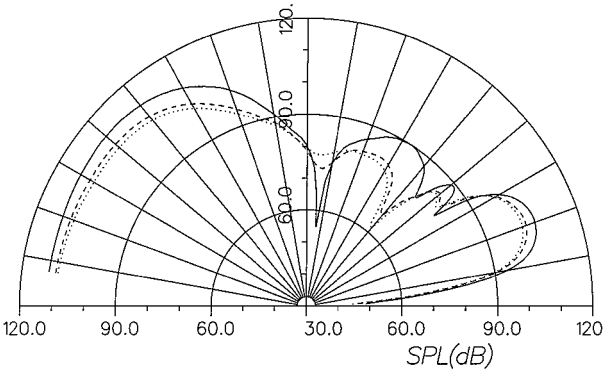

Fig. 17 Computed directivity distributions of the screech tone intensity at $M_j = 1.2$ and $r = 65D$: ——, $t/D = 0.5$; - - -, $t/D = 0.25$; and · · ·, $t/D = 0.125$.

is reproducing the experimental measurements for all three nozzles. This lends confidence in the accuracy of both the experiment and simulation.

Figure 17 shows the computed directivity distributions of the screech-tone intensity at Mach 1.2 scaled to a distance of 65 jet diameters. As can be readily observed, the intensity is only slightly affected by the nozzle-lip thickness. The thick lip nozzle is only 4–5 dB louder. This is consistent with the measurements of Ponton and Seiner,[13] as well as the A_1 mode screech suppression data of Norum.[12]

V. Conclusion

In this work the effects of jet temperature and nozzle-lip thickness on the axisymmetric jet screech modes are investigated by numerical simulation. To establish confidence in the accuracy of the numerical simulation, extensive comparisons of the simulated screech-tone frequencies and intensities with experiments have been done. Good overall agreements are found in all cases. Presently, there is no experimentally measured directivity data. Directivity data are extremely useful in providing a global view of how the screech-tone intensity is affected by a change in jet operating condition or in its surrounding environment. Based on the computed directivities, it is possible to conclude that heated jets emit weaker screech tones. However, the reduction in screech intensity is modest, say, 5 dB when the jet temperature ratio is raised from 1.0 to 2.78. On the other hand, there is a significant increase in screech frequency with temperature. The tone frequency varies like the jet velocity.

We find that nozzle-lip thickness does not have a strong influence on screech intensity over the low supersonic Mach-number range. Our finding is in agreement with the measurements of Ponton and Seiner.[13] We do not find a large increase in tone amplitude by switching from a thin to a thick lip nozzle.

Acknowledgments

This work was supported by NASA John H. Glenn Research Center at Lewis Field Grant NAG 3-2102. Supercomputing time was provided by the U.S. Air Force Wright Laboratory (through Michael Stanek), the SP2 computer of the Supercomputer Computations Research Institute, and the SGI Origin 2000 computer of the Florida State University.

References

[1]Tam, C. K. W., "Supersonic Jet Noise," *Annual Review of Fluid Mechanics*, Vol. 27, 1995, pp. 17–43.

[2]Powell, A., "On the Mechanism of Choked Jet Noise," *Proceedings of the Physical Society, London*, Vol. 66, 1953, pp. 1039–1056.

[3]Tam, C. K. W., "Jet Noise Generated by Large Scale Coherent Motion," *Aeroacoustics of Flight Vehicles: Theory and Practice*, NASA RP-1258, Vol. 1, edited by H. H. Hubbard, 1991, pp. 311–390.

[4]Raman, G., "Advances in Understanding Supersonic Jet Screech," AIAA Paper 98-0279, Jan. 1998.

[5]Rosfjord, T. J., and Toms, H. L., "Recent Observations Including Temperature Dependence of Axisymmetric Jet Screech," *AIAA Journal*, Vol. 13, No. 10, 1975, pp. 1384–1386.

[6]Tam, C. K. W., Ahuja, K. K., and Jones, R. R., III, "Screech Tones from Free and Ducted Supersonic Jets," *AIAA Journal*, Vol. 31, No. 5, 1994, pp. 917–922.

[7]Krothapalli, A., Soderman, P. T., Allen, C. S., Hayes, J. A., and Jaeger, S. M., "Flight Effects on Far-Field Noise of a Heated Supersonic Jet," *AIAA Journal*, Vol. 35, No. 6, 1997, pp. 952–957.

[8]Massey, K. C., and Ahuja, K. K., "Screech Frequency Prediction in Light of Mode Detection and Convection Speed Measurements for Heated Jets," AIAA Paper 97-1625, May 1997.

[9]Massey, K. C., "Flow/Acoustic Coupling in Heated and Unheated Free and Ducted Jets," Ph.D. Dissertation, School of Aerospace Engineering, Georgia Inst. of Technology, Atlanta, March 1997.

[10]Tam, C. K. W., Seiner, J. M., and Yu, J. C., "Proposed Relationship Between Broadband Shock Associated Noise and Screech Tones," *Journal of Sound and Vibration*, Vol. 110, No. 2, 1986, pp. 309–321.

[11]Shen, H., and Tam, C. K. W., "Numerical Simulation of the Generation of Axisymmetric Mode Jet Screech Tones," *AIAA Journal*, Vol. 36, No. 10, 1998, pp. 1801–1807.

[12]Norum, T. D., "Screech Suppression in Supersonic Jets," *AIAA Journal*, Vol. 21, No. 2, 1983, pp. 235–240.

[13]Ponton, M. K., and Seiner, J. M., "The Effects of Nozzle Exit Lip Thickness on Plume Resonance," *Journal of Sound and Vibration*, Vol. 154, No. 3, 1992, pp. 531–549.

[14]Sarkar, S., and Lakshmanan, B., "Application of a Reynolds Stress Model to the Compressible Shear Layer," *AIAA Journal*, Vol. 29, No. 5, 1991, pp. 743–749.

[15]Thies, A. T., and Tam, C. K. W., "Computation of Turbulent Axisymmetric and Nonaxisymmetric Jet Flows using the k–ε Model," *AIAA Journal*, Vol. 34, Vol. 2, 1996, pp. 309–316.

[16]Bogdanoff, D. W., "Compressibility Effects in Turbulent Shear Layers," *AIAA Journal*, Vol. 21, No. 6, 1983, pp. 926, 927.

[17]Papamouschou, D., and Roshko, A., "The Compressible Turbulent Shear Layer: An Experimental Study," *Journal of Fluid Mechanics*, Vol. 197, Dec. 1998, pp. 453–477.

[18]Tam, C. K. W., and Webb, J. C., "Dispersion-Relation-Preserving Finite Difference Schemes for Computational Acoustics," *Journal of Computational Physics*, Vol. 107, Aug. 1993, pp. 262–281.

[19]Tam, C. K. W., "Computational Aeroacoustics: Issues and Methods," *AIAA Journal*, Vol. 33, No. 10, 1995, pp. 1788–1796.

[20]Tam, C. K. W., "Advances in Numerical Boundary Conditions for Computational Aeroacoustics," *Journal of Computational Acoustics*, Vol. 6, Dec. 1998, pp. 377–402.

[21]Norum, T. D., and Brown, M. C., "Simulated High Speed Flight Effects on Supersonic Jet Noise," AIAA Paper 93-4388, Oct. 1993.

P. J. Morris
Associate Editor